Mustansiriyah Journal of Pure and Applied Sciences, Print ISSN: 2957-9910. Online ISSN: 2957-9929, Vol. 4, No. 2, 2026, Pages 111-119
DOI: 10.47831/mjpas.v4i2.345

MJPAS MUSTANSIRIYAH JOURNAL OF PURE AND APPLIED SCIENCES

Journal homepage: https://mjpas.uomustansiriyah.edu.iq/index.php/mjpas

RESEARCH ARTICLE - PHYSICS

Impact of Laser Pulse Variation on the Structural, Morphological, and Optical Properties of Gold Oxide Nanoparticles Synthesized via Laser Ablation Technique

Jamal Aziz[1], Faten Sh. Zainulabdeen[1], R. K. Fakher Alfahed[2*]

[1]Department of Physics, College of Education, Mustanseriyah University, Baghdad, Iraq

[2]Al-Nahrain Renewable Energy Research Center, Al-Nahrain University, Jadriya, Baghdad, Iraq

[*] Corresponding author E-mail: rrr80kkk@nahrainuniv.edu.iq

Article Info.

Article history:

Received
7 November 2024

Accepted
28 January 2025

Publishing
30 June 2026

Abstract

Gold oxide nanoparticles are most useful in various applications due to their distinctive properties. they have valuable photocatalytic, antimicrobial, and optical properties, which makes them very important in antibacterial coatings, sensors, and energy storage applications. This study used the laser ablation technique to synthesize the gold oxide nanoparticles in 2-methoxyethanol. The ablation process was done using a Q-switched Nd:YAG laser with a wavelength of 1064 nm, and different numbers of pulses - 500, 1000, 1500, 2000, and 2500 - were used to irradiate the gold target. Various techniques have been used to characterize the resulting gold oxide nanoparticles, such as FT-IR, to investigate the active groups and bonding patterns. The obtained results noted an interplay between the ablated gold nanoparticles and the surrounding medium. Furthermore, the morphology of prepared nanoparticles was characterized using (AFM), which show that the grain size reduced from 46.7 nm at 500 pulses to be38.3 nm at 2500 pulses. The study also investigated the optical properties by measuring the absorption spectrum at a range of 300-800nm. The energy gap of the acquired colloidal were decreased from 2.73 eV at 500 pulses to 1.34 eV by increasing number of pulses to 2500 pulses.

This is an open-access article under the CC BY 4.0 license (http://creativecommons.org/licenses/by/4.0/)

The official journal published by the College of Education at Mustansiriyah University

Keywords: Nd: YAG laser, Gold oxide, Morphological properties, Energy gap, grain size.

1. Introduction

Nanomaterials have unique properties, including increased surface area and surface activity, which lead to changes in physical properties including the melting factor, as well as quantitative properties including the dielectric constant and effects on solubility and heat transfer [1-2]. Nanomaterial manufacturing techniques are divided into two methods: “top-down” using external forces, and “bottom-up” starting from atoms and molecules [3-4]. Nanoparticles can be produced using rapid pulsed laser ablation, where the material is removed from the target in a liquid medium, reducing the toxicity associated with chemical synthesis [5]. The effectiveness of this method depends on the laser power, the properties of the material, and the wavelength used [6]. Using a high-power laser, the plasma volume increases and the atoms are ionized as the temperature rises to 20,000 K [7-8]. Laser technology is used to produce nanoparticles for a variety of purposes, such as superconductors and laser crystals. Gold nanoparticles have unique optical properties due to surface plasmon resonance, which makes them suitable for use in cancer therapy and most drug delivery systems [12, 13]. Gold nanoparticles are widely used in the fields of biotechnology and biomedicine, due to their special features such as stability, inertness, high anisotropy, biocompatibility and non-toxicity. They have been proven to be one of the safest and least toxic agents for drug delivery [14].

In 2016, Simao and colleagues [15] studied the synthesis of nanoparticles such as gold and manganese oxide via pulsed laser ablation in water, using a nanosecond laser with a wavelength of 248 nm. The test produced nanoparticles with a small gold center surrounded by a layer of manganese oxide, demonstrating the influence of laser parameters on the formation of nanoparticles. In 2018, Torrisi and colleagues [16] compared the synthesis of gold nanoparticles in deionized water and graphene oxide suspensions. The results confirmed that the latter produced Au-rGO nano composites without the need for cleaning agents, thus providing a greener alternative for nanoparticle production. In 2021, Nancy and colleagues [17] synthesized gold oxide-graphene (Au-GO) nanohybrids via pulsed laser ablation in liquid, resulting in gold nanoparticles decorating graphene oxide sheets, demonstrating their effectiveness as systems for surface-enhanced Raman spectroscopy applications. In 2022, Radicic and colleagues [18] studied the synthesis of zinc oxide nanoparticles doped with silver, gold, and platinum using pulsed laser ablation in water, highlighting how gold doping promotes the optical properties and morphology of the resulting nanoparticles.

In this study, gold oxide nanoparticles were produced by pulsed laser ablation method with different number of pulses. High purity gold in 2-methoxyethanol solvent with different number of laser pulses has been targeted. The resulting material was then analyzed and studied for its structural, optical, and morphological properties, as well as the effect of the number of pulses on the shape and size of the nanoparticles.

2. Experimental

2.1. Materials and Characterization Techniques

The materials used in this work include 99% pure gold plate Immersed in 2-methoxyethanol solvent from Sigma Aldrich were used as target and liquid medium respectively. The ablation technique was performed using Nd:YAG laser (. Additionally, the final colloidal were characterized by different techniques such as Atomic Force Microscopy (AFM) (Angstrom AA2000), UV-visible spectrophotometer (UV-1650PC SHIMADZU), and FT-IR Spectrometer (ALPHA).

2.2. Preparation of gold oxide nanoparticles

gold oxide nanoparticles were prepared by pulsed laser ablation (PLA) of a gold plate with a diameter of 5 mm and thickness of 0.05 mm in which the dimensions were measured using a vernier. Subsequently, the gold plate was cleaned ultrasonically for 10 minutes each with ethanol and distilled water to remove surface contaminants effectively. Then fixed in a laboratory tube filled with organic solvent (10 ml of 2-methoxyethanol) and irradiated using a YAG:Nd laser with a wavelength of 1064 nm, pulse duration 9 ns, frequency 9 Hz, and laser power 700 mJ. The target was ablated with different numbers of laser pulses (500, 1000, 1500, 2000, 2500). It is worth noting that the temperature of the laser device must be monitored and controlled so that the operating temperature does not exceed 37 ℃ to keep the device away from damage and defects in the active medium.

The process of synthesizing gold oxide nanoparticles (as illustrated in figure 1) involves exposing a gold target, fixed at the bottom of a laboratory tube filled with an organic solvent, to laser irradiation. This results in rapid heating of the target material, causing it to melt and then evaporate. The evaporation generates a plasma column containing atoms, ions, and electrons, which interact with the surrounding medium to form cavitation bubbles. The significance of these cavitation bubbles lies in the high temperatures and pressures within them, which promote chemical reactions and phase transformations that lead to the formation of nanoparticles. Afterward, the bubbles collapse, releasing the nanoparticles into the surrounding medium.

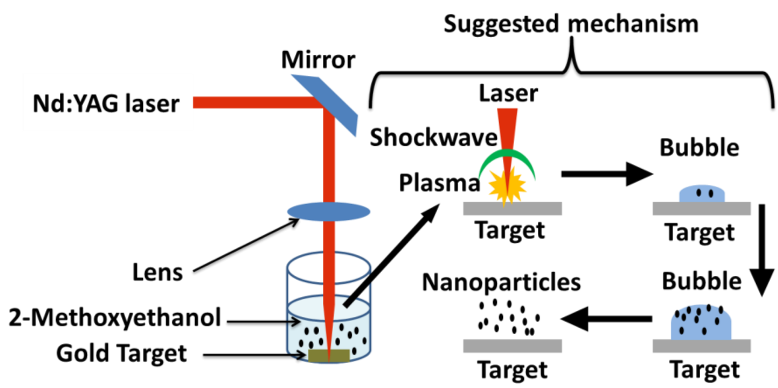

Fig. 1. Synthesis process of the gold oxide nanoparticles

3. Results and Discussion

3.1. FT-IR analysis

FTIR spectroscopy was adopted for analyzing the spectral range of 400-4000 cm^{-1} in order to determine the functional groups of the gold oxide nanoparticles as depicted in Figure 2.Certain peaks' appearance during the synthesis of gold nanoparticles (AuNPs) through laser

ablation in 2-methoxyethanol solution could be explained by energic factors. Nanoparticles and solvent interactions induce vibrational and electronic transitions. Each peak is related to different molecular vibrations or electronic transitions and laser parameters and the chemical environment have an impact on each of these peaks. The peak at 711 cm^{-1} is assigned to C–H bending vibrations of methylene groups which indicate C–H bending vibrations during the interception of the solvent or organic layers adsorbed species [19]. The 803 cm^{-1} peak is attributed to other C–O bending vibrations which are usually found in ethers and these discoveries confirm the presence of a methoxy group in 2-methoxyethanol, which stabilises the nanoparticles [20]. Similarly, the 869 cm^{-1} peak is linked to C–H bending vibrations, suggesting structural changes or interactions on the nanoparticle surface [21]· At 1218 cm^{-1}, C–O stretching vibrations are observed, further supporting the role of the ether functional group in stabilizing AuNPs [22]· The 1382 cm^{-1} peak indicates C–H bending from methyl groups, which may arise from unreacted methoxy groups or organic residues on the surface [23]· The peak at 1605 cm^{-1} can be attributed to C=C stretching vibrations, possibly indicating impurities or degradation products formed during synthesis [24]· The 1743 cm^{-1} peak corresponds to C=O stretching, suggesting oxidation products present in the solution or on the nanoparticle surface [25]· Peaks at 2762 cm^{-1} and 2827 cm^{-1} are associated with C–H stretching vibrations, indicating residual aliphatic hydrocarbons from organic materials in the synthesis process [26]· Finally, the broad peak around 3360 cm^{-1} is refers to O-H stretching vibrations which means presence of hydroxyl groups on the surface of the formed nanoparticles [27-30]All noted peaks through ablated process of nanoparticles gold target refer to interactions between gold target and 2-methoxyethanol solvent. Variations in the number of laser pulses can lead to changes in the size, shape, and oxidation state of nanoparticles, which in turn affect the vibrational and electronic transitions observed in the spectrum. Understanding these peaks is crucial for characterizing nanoparticles and optimizing their formulation for various applications[27-31].

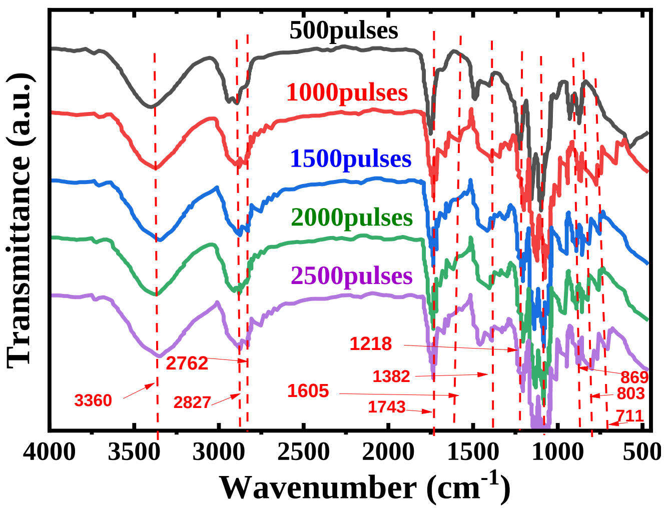

Fig. 2. FTIR spectra of prepared nanoparticles at different numbers of laser pulses.

3.2. Atomic Force Microscope

To study friction, contact deformations, tightness, grain size, and related properties, it is essential to analyze material topography and surface roughness parameters [32-33]. Atomic force microscopy (AFM) is one of the primary techniques used, compared to scanning electron microscopy, as it does not require additional coating layers or staining like in transmission electron microscopy. It also provides three-dimensional images and allows for highly accurate surface morphology studies [34]. In this study, AFM was used to examine the morphological characteristics of gold oxide deposited on glass substrates using the contact mode. The data was analyzed with Gwyddion software. Figure 3 shows the 3D AFM images and the measured grain size distribution, while surface roughness, root mean square, and grain size are listed in Table 1.

As the number of pulses increased, it was observed that both the average roughness and root mean square values varied with the size of the resulting particles. The results indicate that larger grain diameters contribute to greater surface roughness. This observation is consistent with results from previous studies on various nanomaterials synthesized through the laser ablation technique [32]. With varying numbers of laser pulses (500, 1000, 1500, 2000, and 2500), the results show significant fluctuations in the average diameter of the nanoparticles, ranging from 35.8 nm at 2500 pulses to 27.8 nm at 1000 pulses. This variation indicates that the nanoparticle size is directly influenced by the energy imparted by the laser pulses, which can lead to either agglomeration or fragmentation, depending on the pulse count [35-36].

In addition, the Root Mean Square (RMS) roughness, a key measure of surface roughness, varies with the pulse count, reaching its lowest value of 8.6 nm at 1000 pulses and peaking at 3.15nm at 500 pulses. This suggests that the surface morphology of the nanoparticles is highly sensitive to the laser parameters [35, 37]. Similarly, the roughness average follows this pattern, with the lowest value observed of 1.69 nm at 2500 pulses and the highest of 6.93 nm at 1000 pulses, further reinforcing the influence of laser pulses on the surface characteristics of the nanoparticles [35, 38].These findings highlight the profound impact that laser pulse count has on the size, morphology, and surface properties of nanoparticles synthesized through pulsed laser ablation. Optimizing the number of pulses is therefore essential for tailoring the nanoparticle characteristics to meet the requirements of specific applications, such as optoelectronics, catalysis, and biomedical imaging [36-37].

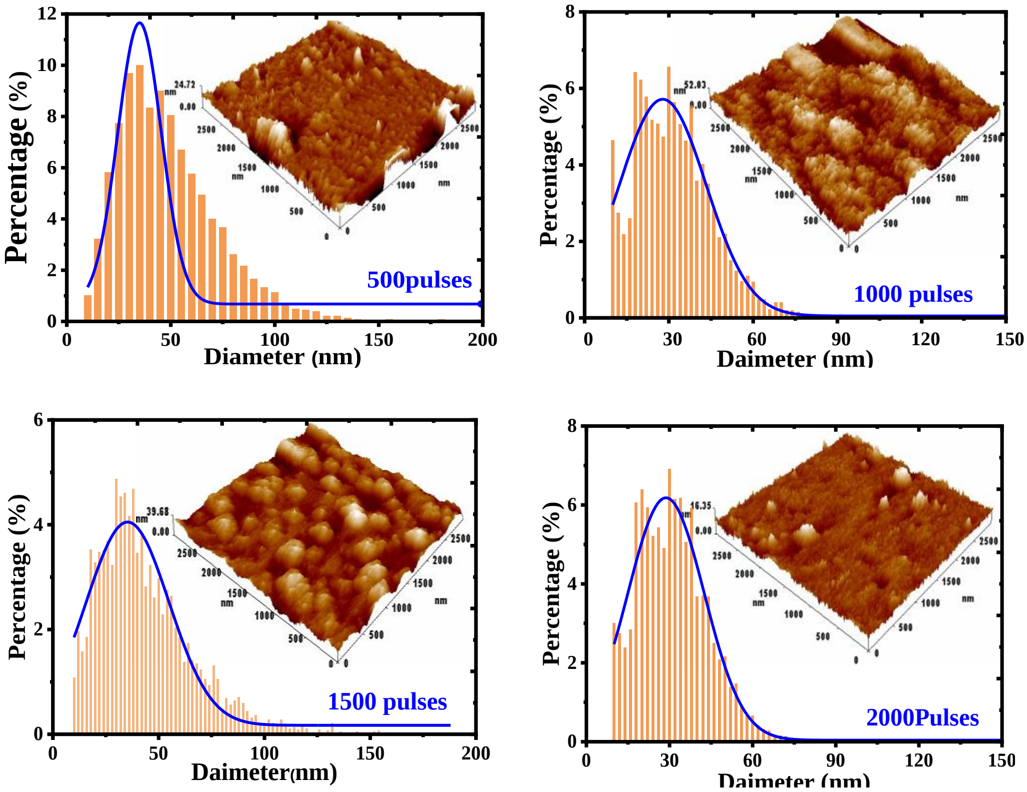

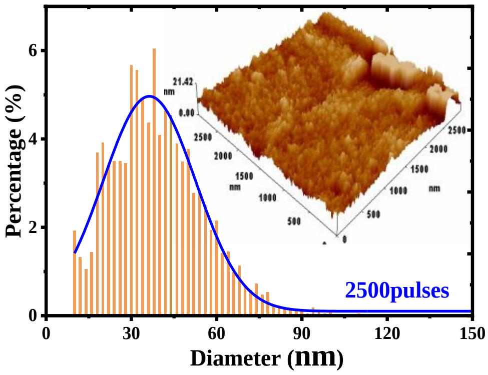

Fig. 3**.** 3D atomic force microscope images of prepared nanoparticles.

Table 1. Atomic force microscope parameters of prepared nanoparticles

Sample	Average Diameter (nm)	Root Mean Square RMS (nm)	Roughness Average (nm)
Au-500 Pulses	34.9	3.15	2.07
Au-1000 Pulses	27.8	8.6	6.93
Au-1500 Pulses	35.1	5.46	4.29
Au-2000 Pulses	28.6	6.94	5.47
Au-2500 Pulses	35.9	2.66	1.99

3.3. UV-Visible analysis

The Colloidal phase of the prepared nanoparticles in suspension was examined through optical absorption measurements for a wavelength range of 300-800 nm. The measured spectra are illustrated in Fig. 4a.
the spectra show broad absorption peaks centered at 572 nm and 350 nm. The 572 nm peak is associated with the gold nanoparticles' surface plasmon resonance (SPR) which arises from the oscillation of conduction electrons in unison upon exposure to light. This peak is induced by the surface plasmon resonance (SPR) in the gold nanostructures. The SPR peak depends on the dimension and form of the nanoparticles, with the former being typically red-shifted by increasing size, with the latter normally being blue-shifted by the opposite effect [39]. The peak at 350 nm is commonly attributed to residual gold ions or byproducts from incomplete reduction of gold precursors [40]. Additionally, the number of laser pulses plays a crucial role in determining the properties of the nanoparticles. Increasing the number of pulses enhances energy transfer, resulting in more efficient ablation and potentially larger or more uniform nanoparticles [41]. Variations in synthesis conditions, particularly pulse count, lead to significant differences in the UV-Vis spectra, notably affecting the intensity and position of the SPR peak at 572 nm. Thus, optimizing the number of pulses is essential to produce nanoparticles with tailored optical properties [42].

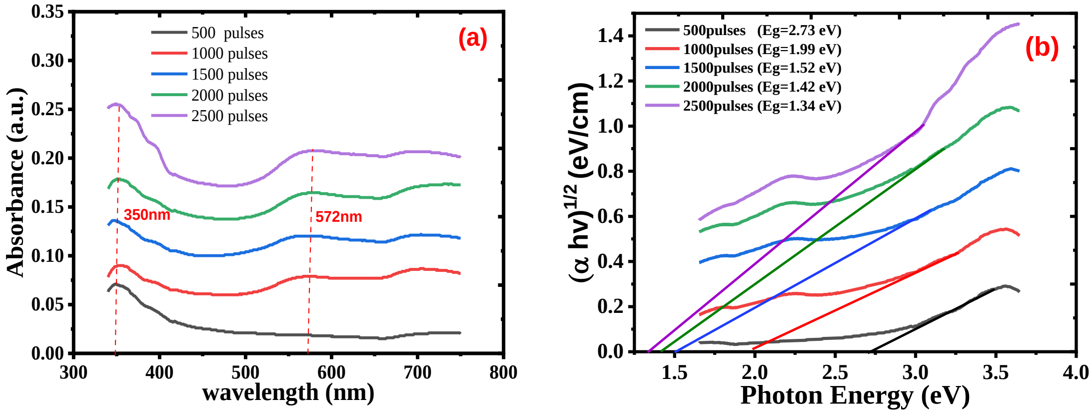

Fig. 4. UV-visible spectra of nanoparticles. **(a)** absorbance spectra, **(b)** Plot of $(\alpha hv)^{1/2}$ versus photon energy.

The estimated values of the indirect band gap for gold nanoparticles prepared using the laser ablation technique range between 2.73 and 1.34 eV as the number of pulses increases from 500 to 2500, as shown in Figure 4b. The band gap has been calculated according to Tauc's relation [43-44]. The decrease in the band gap can be explained by several factors. First, the quantum confinement effect plays a significant role in determining the properties of the particles; smaller nanoparticles are formed due to the increased number of pulses, leading to a larger band gap due to quantum confinement, where larger particles are associated with a larger band gap [45]. Second, electron-phonon interactions contribute to the appearance of an absorption edge on the lower side of the spectrum, corresponding to a smaller band gap. Additionally, the Tauc plot analysis is a reliable method for determining the band gap values of gold nanoparticles, with studies showing values ranging from 2.74 to 3.50 eV for gold nanoparticles prepared using the laser ablation technique [46]. Therefore, the decrease in the indirect band gap of gold nanoparticles with an increasing number of pulses is attributed to the quantum confinement effect, where smaller particles formed from more pulses lead to a larger band gap [45].

Conclusion

In this work, YAG:Nd laser with a wavelength of 1064 nm, pulse duration 9 ns, frequency 9 Hz, and laser power 700 mJ has been used to synthesis gold oxide nanoparticles by laser ablation method. the obtained nanoparticles were subjected for various techniques to investigate their properties. the infrared spectroscopy was utilized the functional groups of gold oxide nanoparticles. All noted peaks through the ablated process of nanoparticles gold target refer to interactions between gold target and 2-methoxyethanol solvent. Moreover, Increasing the number of pulses from 500 to 2500 pulse led to a decrease in the grain size from 46.7 to 38.3 nm, which led to a decrease in the average roughness and root mean square ratio. The lower roughness values at higher pulse counts indicate a more uniform surface morphology. The optical absorption of the colloidal suspension phase of the prepared nanoparticles was analyzed within the wavelength range of 300–800 nm. The absorption peaks were noted at 572 nm and 350 nm corresponding to the effect of surface plasmon resonance (SPR) and the formation of gold oxide nanoparticles respectively. Furthermore, the energy gap was decreased with increasing number of laser pulses has been reported. Starting from say 2.73 eV at 500 pulses to 1.34 eV at 2500 pulses.

References

[1] K. Alaqad and T. A. Saleh, "Gold and silver nanoparticles: synthesis methods, characterization routes and applications towards drugs," *J. Environ. Anal. Toxicol*, vol. 6, pp. 525-2161, 2016, doi: 10.4172/2161-0525.1000384.

[2] M. Ahmeda, N. Ahmida, and A. Ahmeida, "Introduction to nanotechnology: definition, terms, occurrence and applications in environment," *Libyan International Medical University Journal*, vol. 2, p. 12, 2017, doi: 10.21502/limuj.003.02.2017.

[3] K. D. Sattler, *Handbook of nanophysics: nanoparticles and quantum dots*: CRC press, Taylor & Francis Group, LLC, 2011.

[4] A. J. Aswad, S. J. Fathi, and R. M. S. Al-haddad, "Study optical and structural propertiesof copper oxide nanoparticles prepared by pulse laser ablation technology in (LC/MS) water,", *Kirkuk University Journal /Scientific Studies (KUJSS)*, vol.12, Issue 1, January 2017, ISSN 1992 – 0849.

[5] F. A. Mytlak, "Synthesis and characterization of Au nanoparticles for nanomedicine application," *Iraqi Journal of Physics (IJP)*, vol. 15, pp. 109-116, 2017.

[6] K. Sugioka, M. Meunier, and A. Piqué, *Laser precision microfabrication*: Springer Series in Materials Science, vol. 135, 2010, doi 10.1007/978-3-642-10523-4_2.

[7] N. Kumar, S. Dash, A. Tyagi, and B. Raj, "Dynamics of plasma expansion in the pulsed laser material interaction," *Sadhana*, vol. 35, pp. 493-511, 2010.

[8] R. Bernath, C. G. Brown, J. Aspiotis, M. Fisher, M. Richardson, "Shock-wave generation in transparent media from ultra-fast lasers," *Proc. SPIE 6219, Enabling Technologies and Design of Nonlethal Weapons*, 62190A (26 May 2006); doi: 10.1117/12.663818.

[9] S. Link, C. Burda, Z. L. Wang, and M. A. El-Sayed, "Electron dynamics in gold and gold–silver alloy nanoparticles: The influence of a nonequilibrium electron distribution and the size dependence of the electron–phonon relaxation," *The Journal of chemical physics*, vol. 111, pp. 1255-1264, 1999.

[10] S. J. Hill, "*Inductively coupled plasma spectrometry and its applications"* , 2nd Edition, Wiley-Blackwell, 448 pages, November 2007.

[11] J. A. Grant-Jacob, S. J. Beecher, T. L. Parsonage, P. Hua, J. I. Mackenzie, D. P. Shepherd, *et al.*, "An 11.5 W Yb: YAG planar waveguide laser fabricated via pulsed laser deposition," *Optical Materials Express*, vol. 6, pp. 91-96, 2016.

[12] M. A. K. Abdelhalim, M. M. Mady, and M. M. Ghannam, "Physical properties of different gold nanoparticles: ultraviolet-visible and fluorescence measurements," *J. Nanomed Nanotechol*, vol. 3, pp. 178-194, 2012.

[13] R. K. I. AL-Ageedie, "Surface Plasmon Resonance of Gold and Silver Nanoparticles for Biomedical Physics Applications," *PhD Thesis, College of Science, University of Diyala, Iraq.*, 2019.

[14] E. Y. Lukianova-Hleb, D. S. Wagner, M. K. Brenner, and D. O. Lapotko, "Cell-specific transmembrane injection of molecular cargo with gold nanoparticle-generated transient plasmonic nanobubbles," *Biomaterials*, vol. 33, pp. 5441-5450, 2012.

[15] Simão, T.S., Chevrier, D.M., Jakobi, J., Korinek, A., Goupil, G., Lau, M., Garbarino, S., Zhang, P., Barcikowski, S., Fortin, M., & Guay, D. (2016). Gold–Manganese Oxide Core–Shell Nanoparticles Produced by Pulsed Laser Ablation in Water. *Journal of Physical Chemistry C, 120*, 22635-22645.

[16] Torrisi, L., Cutroneo, M., Silipigni, L., Barreca, F., Fazio, B., Restuccia, N.L., & Kovacik, L. (2018). Gold nanoparticles produced by laser ablation in water and in graphene oxide suspension. *Philosophical Magazine, 98*, 2205 - 2220.

[17] Nancy, P., Thomas, S., & Kalarikkal, N. (2021). Au-GO nanohybrids as SERS platforms fabricated via pulsed laser ablation. *NATIONAL CONFERENCE ON PHYSICS AND CHEMISTRY OF MATERIALS: NCPCM2020*.

[18] Radičić, R., Maletić, D., Blažeka, D., Car, J., & Krstulović, N. (2022). Synthesis of Silver, Gold, and Platinum Doped Zinc Oxide Nanoparticles by Pulsed Laser Ablation in Water. *Nanomaterials (Basel, Switzerland)*, *12*(19), 3484. https://doi.org/10.3390/nano12193484.

[19] Subaer, S., Hartati, H., Ramadhan, I., Ismayanti, H., & Setiawan, A. (2023). A Simple Synthesis and Microstructure Analysis of Human Peptide LL-37@Gold Nanoparticles (Known as LL-37@AuNPs) Conjugates as Antimicrobials and Substances for Wound Healing. *Materials (Basel, Switzerland)*, *16*(24), 7675. https://doi.org/10.3390/ma16247675

[20] Li, X., Yu, H., Wang, B., Chen, W., Zhu, M., Liang, S., Chu, R., Zhou, S., Chen, H., Wang, M., Zheng, L., & Feng, W. (2021). Multiscale Synchrotron-Based Imaging Analysis for the Transfer of PEGylated Gold Nanoparticles *In Vivo*. *ACS biomaterials science & engineering*, *7*(4), 1462–1474. https://doi.org/10.1021/acsbiomaterials.0c01764

[21] Ullah, R., Bibi, S., Khan, M.N., Al Mohaimeed, A.M., Naz, Q., & Kamal, A. (2023). Application of Bio-Inspired Gold Nanoparticles as Advanced Nanomaterial in Halt Nociceptive Pathway and Hepatotoxicity via Triggering Antioxidation System. *Catalysts*.

[22] Gawas, G., Ayyanar, M., Gurav, N., Hase, D., Murade, V., Nadaf, S., Khan, M. S., Chikhale, R., Kalaskar, M., & Gurav, S. (2023). Process Optimization for the Bioinspired Synthesis of Gold Nanoparticles Using *Cordyceps militaris*, Its Characterization, and Assessment of Enhanced Therapeutic Efficacy. *Pharmaceuticals (Basel, Switzerland)*, *16*(9), 1311. https://doi.org/10.3390/ph16091311

[23] Hasoon, B.A., Jawad, K.H., & Abdulsahib, S.S. (2023). Synthesis of Ciprofloxacin-Conjugated Gold Nanoparticles and their Study Antibacterial Effects on Growth Biofilm Formation Through Nebulizer Mask Against Respiratory Infection. *Plasmonics*, 1-15.

[24] Anisuzzman, M., Komalla, V., Tarkistani, M. A. M., & Kayser, V. (2023). Anti-Tumor Activity of Novel Nimotuzumab-Functionalized Gold Nanoparticles as a Potential Immunotherapeutic Agent against Skin and Lung Cancers. *Journal of functional biomaterials*, *14*(8), 407. https://doi.org/10.3390/jfb14080407

[25] Kumar, D., Moghiseh, M., Chitcholtan, K., Mutreja, I., Lowe, C., Kaushik, A., Butler, A., Sykes, P., Anderson, N., & Raja, A. (2023). LHRH conjugated gold nanoparticles assisted efficient ovarian cancer targeting evaluated *via* spectral photon-counting CT imaging: a proof-of-concept research. *Journal of materials chemistry. B*, *11*(9), 1916–1928. https://doi.org/10.1039/d2tb02416k

[26] Zainol Abidin, N. A., Kormin, F., Zainol Abidin, N. A., Bakar, M. F. A., & Moujdin, I. A. (2023). Synthesis and Characterization of Curcumin-Chitosan Loaded Gold Nanoparticles by *Oryctes rhinoceros'* Chitin for Cosmeceutical Application. *Molecules (Basel, Switzerland)*, *28*(4), 1799. https://doi.org/10.3390/molecules28041799

[27] Jasim, A. S., & Mahmood, A. S. (2023). Preparation of Copper Nanoparticles Using Different Media by Pulsed Laser Ablation and Study of Their Physical Properties. *Journal for Research in Applied Sciences and Biotechnology*, *2*(4), 122-125.

[28] Mulder, A. J., Tilbury, R. D., Werrett, M. V., Wright, P. J., Patel, P., Becker, T., ... & Buntine, M. A. (2023). Ligand-mediated control of the surface oxidation states of copper nanoparticles produced by laser ablation. Langmuir, 39(14), 5156-5168.

[29] Ajaj, K., Al-Jubbori, M. A., & Ali, A. M. (2023). Influence of ultraviolet irradiation on the optical properties and biological activity of copper nanoparticles prepared by pulsed laser ablation. Journal of Laser Applications, 35(4).

[30] Miao, R., Bissoli, M., Basagni, A., Marotta, E., Corni, S., & Amendola, V. (2023). Data-Driven Predetermination of Cu Oxidation State in Copper Nanoparticles: Application to the Synthesis by Laser Ablation in Liquid. Journal of the American Chemical Society, 145(47), 25737-25752.

[31] A. Shepelev, A. Antipov, A. Putilov, S. Solokhin, and T. Lezova " International Scientific Conference Energy Management of Municipal Facilities and Environmental Technologies (EMMFT-2023) " E3S Web of Conferences **458**, 02032 (2023).

[32]Alfahed, R. F., Imran, A., Badran, H. A., & Al-Salihi, A. (2020). Synthesis, optical limiting behavior, thermal blooming and nonlinear studies of dye-doped polymer films. Journal of Materials Science: Materials in Electronics, 31(16), 13862-13873.

[33] Alfahed, R. K. F., Alameri, D., Yassar, Z., Badran, H. A., & Mohammad, K. K. (2023). Preparation and characterization of tin chloride-based polymeric composite for gamma shielding applications. Applied Radiation and Isotopes, 196, 110774.

[34]R. K. F. Alfahed1, K. K. Mohammad, M. S. Majeed, H. A. Badran, K. M. Ali, B. Y. Kadem "First International Scientific Conference Al-Ayen University" Journal of Physics: Conf. Series 1279, 012019 (2019).

[35] Gezgin, S. Y., Kepceoğlu, A., & Kılıç, H. Ş. (2017, February). An experimental investigation of localised surface plasmon resonance (LSPR) for Cu nanoparticles depending as a function of laser

pulse number in Pulsed Laser Deposition. In *AIP Conference Proceedings* (Vol. 1815, No. 1). AIP Publishing

[36]Chiad, B. T., Mutlak, F. A., Ahamed, L. S., & ALI, M. H. Production of Au NPs via PLAL Technique for Optoelectronic Application.

[37]Naranji, E., Aliannezhadi, M., & Panahibakhsh, S. (2023). Surface structured silver-copper bimetallic nanoparticles by irradiation of excimer laser pulses to bilayer thin films. *Physica Scripta*, *98*(10), 105529.

[38] Subhan, A., Mourad, A. H. I., & Al-Douri, Y. (2022). Influence of laser process parameters, liquid medium, and external field on the synthesis of colloidal metal nanoparticles using pulsed laser ablation in liquid: A review. *Nanomaterials*, *12*(13), 2144.

[39] Ali, H. S., Fakhri, M. A., & Khalifa, Z. (2021, March). Optical and structural properties of the gold nanoparticles ablated by laser ablation in ethanol for biosensors. In *Journal of physics: conference series* (Vol. 1795, No. 1, p. 012065). IOP Publishing.

[40] Naser, H., Shanshool, H. M., & Imhan, K. I. (2021). Parameters affecting the size of gold nanoparticles prepared by pulsed laser ablation in liquid. *Brazilian Journal of Physics*, *51*(3), 878-898.

[41] Mzwd, E., Ahmed, N. M., Suradi, N., Alsaee, S. K., Altowyan, A. S., Almessiere, M. A., & Omar, A. F. (2022). Green synthesis of gold nanoparticles in Gum Arabic using pulsed laser ablation for CT imaging. *Scientific Reports*, *12*(1), 10549.

[42] Shukri, W. N. W., Bidin, N., Affandi, S., & Bohari, S. P. (2016). Synthesize of gold nanoparticles with 532 NM and 1064 NM pulse laser ablation. *Jurnal Teknologi*, *78*(3).

[43] W. M. Taher, Z. M. Abood ,A. A. Khadayier, (2024). Investigating the Structural and Optical Properties of Pure and Zinc (Zn)-Doped Copper Oxide at Different Weight Ratios, *MUSTANSIRIYAH JOURNAL OF PURE AND APPLIED SCIENCES*, 2, 49-58.

[44] A. J. Mohammed , S. A. Hamdan, (2024). Study the Effect of Calcined Temperature on Structural, Optical and Magnetic Properties for Cobalt Ferrite Nanostructure, MUSTANSIRIYAH JOURNAL OF PURE AND APPLIED SCIENCES, 2, 116-135.

[45] Tommalieh, M. J., Ismail, A. M., Awwad, N. S., Ibrahium, H. A., Youssef, M. A., & Menazea, A. A. (2020). Investigation of electrical conductivity of gold nanoparticles scattered in polyvinylidene fluoride/polyvinyl chloride via laser ablation for electrical applications. *Journal of Electronic Materials*, *49*, 7603-7608.

[46] Abdelghany, A. M., Elashmawi, I. S., Al-Shamari, A. A., & Alnattar, H. (2023). Dielectric behavior and AC conductivity of PEO/CMC polymer blend incorporated with gold nanoparticles produced by laser ablation. *Journal of Materials Science: Materials in Electronics*, *34*(5), 388.